

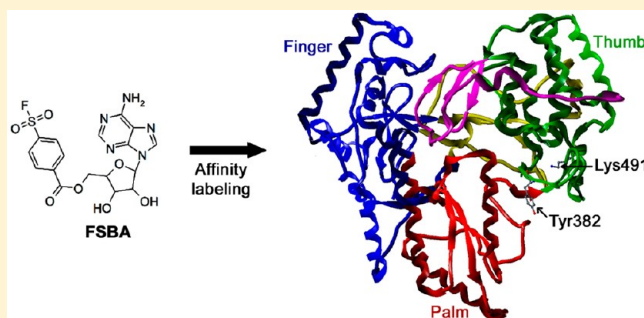
Affinity Labeling of Hepatitis C Virus Replicase with a Nucleotide Analogue: Identification of Binding Site

Dinesh Manvar, Kamendra Singh, and Virendra N. Pandey*

Department of Biochemistry and Molecular Biology, New Jersey Medical School, University of Medicine and Dentistry of New Jersey, Newark, New Jersey 07103, United States

Supporting Information

ABSTRACT: We have used an ATP analogue 5'-[p-(fluorosulfonyl)benzoyl]adenosine (FSBA) to modify HCV replicase in order to identify the ATP binding site in the enzyme. FSBA inactivates HCV replicase activity in a concentration-dependent manner with a binding stoichiometry of 2 moles of FSBA per mole of enzyme. The enzyme activity is protected from FSBA in the presence of rNTP substrates or double-stranded RNA template primers that do not support ATP as the incoming nucleotide but not in the presence of polyU.rA₂₆. HPLC analysis of tryptic peptides of FSBA-modified enzyme revealed the presence of two distinct peptides eluted at 23 and 36 min; these were absent in the control. Further we noted that both peptides were protected from FSBA modification in the presence of Mg-ATP. The LC/MS/MS analysis of the affinity-labeled tryptic peptides purified from HPLC, identified two major modification sites at positions 382 (Tyr), and 491 (Lys) and a minor site at position 38 (Tyr). To validate the functional significance of Tyr38, Tyr382, and Lys491 in catalysis, we individually substituted these residues by alanine and examined their ability to catalyze RdRp activity. We found that both Y382A and K491A mutants were significantly affected in their ability to catalyze RdRp activity while Y38A remained unaffected. We further observed that both Y382A and K491A mutants were not affected in their ability to bind template primer but were significantly affected in their ability to photo-cross-link ATP in the absence or presence of template primer.



HCV is currently the major cause of chronic liver disease, with approximately 3% of the world's population estimated to be infected with the virus.¹ Although some infected individuals are able to clear the virus without treatment, most infections persist if untreated, leading to chronic hepatitis C, which may further lead to liver cirrhosis and hepatocellular carcinoma.² Current therapy for HCV infection includes extended administration of a combination of ribavirin and pegylated interferon- α .^{3–5} However, this combination produces sustained virological response of approximately 40–50% in genotype 1-infected individuals but does not show similar response in other genotypes.^{6,7} Recently, the FDA approved use of the protease inhibitors, Boceprevir and Telaprevir, which in combination with ribavirin and pegylated interferon- α demonstrated a cure rate of 60–80% for genotype 1 patients^{8–10} and thus offer a new treatment option for the patients who failed to respond conventional treatment.¹¹ However, these inhibitors have showed some serious side effects in clinical trials.^{10,12}

HCV is a (+) strand RNA virus having a genome size that is approximately 9.6 kb long and contains a single long open-reading frame encoding a polyprotein of approximately 3000 amino acids. The structural proteins are located at the N-terminal portion, followed by nonstructural proteins. The genomic HCV (+) strand RNA is first copied into (–) strand HCV RNA, which is then used as the template to produce a large number of progeny (+) strand RNA. One of the

nonstructural proteins is HCV replicase (NS5B), which contains RNA-dependent RNA polymerase activity (RdRp) and is responsible for replicating the viral RNA.^{13,14} NS5B is a 68-kDa protein that can carry out RNA synthesis on primed RNA template, as well as de novo synthesis of viral RNA in the absence of primer. However, the detailed mechanism of RdRp and de novo initiation steps remain unclear.

Many crystal structures of HCV NS5B have been reported.^{15–20} Like three-dimensional structures of other polymerases, HCV replicase is folded into fingers, palm, and thumb domains resembling a right-hand structure.^{16,17} Unlike DNA polymerases with an open polymerase cleft, HCV NS5B is crystallized in closed conformation with a $\Delta 1$ finger loop anchored into the hydrophobic pocket on the thumb, thus closing the polymerase cleft.²¹ A similar closed conformation has been reported for other RNA replicases.²² The closed conformation assumes open conformation during the formation of active polymerase complexes.²³ Crystal structure of HCV NS5B from the genotype 2a strain has been reported to exist in open and closed conformation, which is proposed to represent, respectively, inactive and active forms of the enzyme.²⁰ Since

Received: August 14, 2012

Revised: December 21, 2012

Published: December 27, 2012



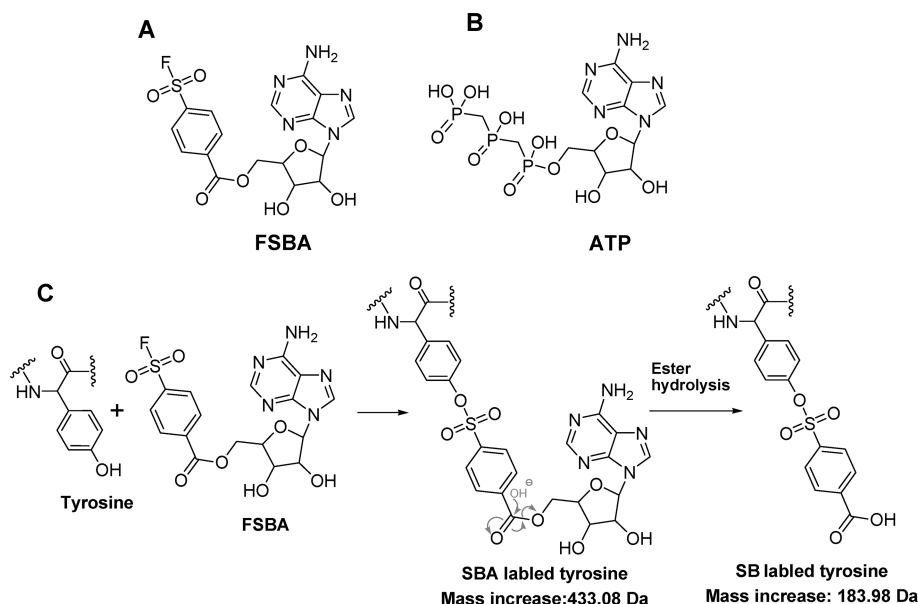


Figure 1. (A) Chemical structure of FSBA. (B) Chemical structure of ATP. (C) Reaction scheme of tyrosine modification by FSBA is shown as a representative of FSBA linked to peptide. SBA and SB add masses of 433.08 and 183.98 Da, respectively.

both conformations lack bound RNA template or NTP substrate, it is yet to be determined whether binding of RNA template or substrate will induce similar structural change. HCV replicase in solution has been shown to exist in both monomeric and oligomeric forms.^{24–29} Using real-time ultracentrifugation analyses, it has been shown that HCV NSSB is predominantly monomeric in solution and can be induced into oligomeric form by short RNA templates.²⁷ It has been suggested that the oligomeric form of HCV NSSB is critical for catalyzing RdRp activity.^{24,25,28,30,31} Moreover, Bressanelli et al. suggested that the closed structure of NSSB represents a “preformed active site” in the absence of template.¹⁸

Studies have proposed that HCVNSSB undergoes a transition to an open structure to accept the template RNA.^{20,32–34} This contention is supported by experiments in which a circular template has been shown to be used by HCV NSSB, suggesting that the “closed” polymerase cleft of the enzyme may open up to accommodate the circular template.²³ Bressanelli et al. have cocrystallized NSSB with GTP, showing that GTP interacts with four residues in the thumb subdomain and two residues on the $\Delta 1$ finger tips.¹⁸ Binding of GTP to the enzyme also has been proposed to stabilize the interaction of $\Delta 1$ finger tips and thumb domain, thus favoring monomeric conformation. The interacting sites on the thumb and fingertips are both on the surface of the enzyme molecule, located 30 Å away from the polymerase active site residues Asp318, Asp319, and Asp220. Since NSSB may undergo significant conformational changes during the transition from initiation to elongation, it is expected to exist in multiple conformations. In this study, we used fluorosulfonyl benzoyl adenosine as an NTP analogue for affinity labeling of HCV NSSB to map the NTP binding site(s) on the enzyme molecule. This analogue has been used successfully to probe the nucleotide binding site(s) in polymerases and kinases.^{35–43} The structure and size of FSBA are such that it resembles ATP, and its reactive sulfonyl fluoride moiety may reside in the positions of β and γ phosphate of NTP (Figure 1). The reactive sulfonyl fluoride group of FSBA reacts with the nucleophilic side chain of amino

acid residues in the vicinity of the nucleotide binding domain (NBD) of the enzyme.

MATERIALS AND METHODS

IDA-Sepharose for immobilized metal affinity chromatography (IMAC) was obtained from Pharmacia. HPLC purified ultrapure NTPs were purchased from Roche Applied Sciences. FSBA and synthetic template-primers were from Sigma-Aldrich. Mass spectrometry grade trypsin was obtained from Promega. The [³H] labeled FSBA was prepared as described⁴⁴ and freshly dissolved in DMSO before use. A site-directed mutagenesis kit (QuickChange) was purchased from Stratagene. All reagents, purchased from Fisher, Millipore and Bio-Rad, were of the highest available purity. Fluorescence quenching was done on a Varian Cary Eclipse fluorescence spectrophotometer. GraphPad Prism 4.0 (GraphPad software) was applied for plotting the data using nonlinear fit to the data using hyperbolic function. The pET21C-SB Δ 21 plasmid expressing His-tagged HCV NSSB with 21 amino acid deletion from the C terminal was a gift from Dr. Sergey Kochetkov.⁴⁵

Expression and Purification of HCV NSSB and in Vitro Mutagenesis. The pET21C-SB Δ 21 expression clone of HCV NSSB was expressed in *Escherichia coli* Rosetta (DE3), as described.⁴⁵ In brief, the transformed cells were grown with vigorous shaking at 37 °C in Luria Broth containing 100 mg/L ampicillin and 15 mg/L chloramphenicol to a density of 0.4 at 595 nm. NSSB expression was induced by the addition of 1 mM IPTG. The cells were further incubated at 25 °C with vigorous shaking for 4 h. The cells were harvested and lysed; His-tagged HCV NSSB was purified on an IMAC column. The eluted fractions containing small impurities were further purified on FPLC (Pharmacia) using a prepacked 1 mL Hi-Trap Heparin column (Pharmacia). In brief, the IMAC fractions were pooled and diluted 3-fold with buffer A (100 mM Tris HCl (pH 7.0), 5% glycerol, 0.5% triton X-100, and 1 mM β -mercaptoethanol) and loaded onto the Hi-Trap Heparin column. After the column was washed with 2 column volumes of buffer A, the enzyme was eluted with a linear gradient (0% to 80%) of 1 M KCl in the same buffer in 20 min (1 mL/min).

Eluted fractions showing more than 98% purity on SDS-PAGE (8%) were collected and stored at -80°C in a buffer containing 50 mM Tris HCl (pH 7.8), 1 mM DTT, 100 mM NaCl, and 50% glycerol. Site-directed mutagenesis was carried out using the QuickChange mutagenesis kit according to the manufacturer's protocol. Mutations were confirmed by sequencing at the UMDNJ Molecular Resource Facility.

Fluorescence Quenching Assay. The fluorescence-quenching (FQ)-based binding assay was done in a final volume of 100 μL per well in a 96-well plate (Fluotrac 200). HCV NSSB (1 μM) was incubated in the absence and presence of FSBA in a buffer containing 50 mM Tris HCl (pH 7.8), 50 mM NaCl, 10% glycerol, 10% DMSO, and 0.5 mM MnCl_2 . The mixture was incubated at room temperature for 20 min. The fluorescence emission of enzyme control or enzyme-ligand complex was monitored at 300–420 nm with an excitation wavelength of 280 nm. The emission fluorescence intensity of HCV NSSB in the absence and presence of FSBA had the same fluorescence emission maxima, at 330 nm, suggesting that enzyme bound with FSBA did not shift the emission wavelength.

RdRp Assay. This assay was done at 37°C in a total volume of 25 μL containing 20 mM Tris HCl (pH 7.8), 40 mM NaCl, 40 mM sodium glutamate, 0.5 mM DTT, 0.01% BSA, 0.01% tween-20, 5% glycerol, 20 U/mL RNase Out, 25 μM cold UTP, 1 μCi /assay ^3H UTP or $\alpha^{32}\text{P}$ UTP, 500 nM PolyA.dT₁₈ and 0.5 mM MnCl_2 . The reaction was started by the addition of 588 nM HCV NSSB and terminated by the addition of 5% ice cold trichloroacetic acid. The terminated reaction mixture was kept on ice for 30 min, after which acid-insoluble material was filtered on glass fiber filters (GF/B). The filters were washed with 5% TCA, water, and ethanol. Filters were dried under infrared lamp and placed in vials containing 5 mL EcoLite scintillation fluid. Radioactivity was counted on a Packard 2200-CA Tri-Carb scintillation counter.

Inactivation of NSSB by FSBA. HCV NSSB (3 μM) was preincubated with varying concentrations of FSBA in a buffer containing 20 mM Tris HCl (pH 7.8), 40 mM NaCl, 40 mM sodium glutamate, 0.01% tween-20, 5% glycerol, and 10% DMSO in a final volume of 100 μL . An aliquot of the incubation mixture was withdrawn periodically and assayed for RdRp activity.

Stoichiometric of FSBA Binding to NSSB. For determining the binding stoichiometry, we used [^3H]-labeled FSBA. We incubated 4 μM of NSSB in the presence of varying concentrations of [^3H]-FSBA (0.25 mM to 1 mM) as above in the incubation buffer in a total volume of 500 μL . Aliquots were withdrawn periodically and spotted on Whatman chromatography paper strip #3 and subjected to ascending chromatography using methanol/chloroform (1:1) as the mobile phase. Free [^3H]-FSBA was migrated near the solvent front, whereas [^3H]-SBA bound to NSSB remained at the origin. After 1 h, the chromatography strip was removed, air-dried and ^3H radioactivity remaining at the point of application was determined by liquid scintillation counting. A sample containing the standard reaction mixture minus the enzyme was also incubated similarly, and the enzyme was added to this mixture just before spotting on the chromatography paper strip. The ^3H count obtained at the origin was used as the background.

5'- ^{32}P Labeling of Oligomeric Primer or Template Primer. 37-mer double-stranded RNA looped template primer and dT₁₈ primer were labeled at 5' using [$\alpha^{32}\text{P}$]ATP and T4 polynucleotide kinase (Invitrogen) according to manufacturer's

protocol. The 5' labeled oligomers were purified by illustra ProbeQuant G-50 micro columns.

Photo-Cross-Linking of Double-Stranded Template Primers to HCV NSSB. Two micromoles of HCV NSSB or its mutant derivatives were incubated on ice with 20 nM of 5'- ^{32}P labeled 37-mer double-stranded looped RNA template primer (Chart S1) or poly rA.5'- ^{32}P -dT₁₈ (20K Cerenkov CPM) in a cross-linking buffer containing 20 mM Tris HCl (pH 7.8), 40 mM NaCl, 40 mM sodium glutamate, 2 mM DTT and 0.5 mM MnCl_2 in a final volume of 50 μL . After 20 min incubation, samples were irradiated by UV light at 254 nm, with a dose rate of 3600 J/m² (Spectrolinker XL-1000) at a distance of 10.5 cm. The irradiated samples were mixed with gel loading dye and resolved by SDS-PAGE using 8% polyacrylamide gel. The cross-linked enzyme-TP complexes were visualized by phosphorImager and gels were stained using Coomassie blue staining.

Photo-Cross-Linking of [$\alpha^{32}\text{P}$]-ATP with HCV NSSB and Its Mutant Derivatives in the Binary and Ternary Complex. The wild type HCV NSSB or its mutant derivatives (7 μg) was incubated with 20 μCi [$\alpha^{32}\text{P}$]-ATP in the cross-linking buffer in the absence or presence of 2 μM of preannealed rU₁₅.rA₁₀ template primer with 3'-deoxy terminated primer terminus. After 20 min incubation on ice, the mixture was UV irradiated as above and the cross-linked complexes were resolved by SDS-PAGE and visualized by autoradiography.

Nucleotidyl Transferase Activity of the Enzyme Cross-Linked with Double-Stranded RNA Template Primer.

Two micromoles of HCV NSSB was incubated with 2 μM of unlabeled 37-mer double-stranded RNA template primer (Chart S1) by UV irradiation as described above. An aliquot of the cross-linked enzyme-TP binary complex was incubated with 10 μCi $\alpha^{32}\text{P}$ UTP in a reaction mixture containing 20 mM Tris HCl (pH 7.8), 0.5 mM DTT and viable salt concentration ranging from 50 mM to 1 M in a final volume of 50 μL . The mixture was incubated at 37°C for 30 min and the incorporation of ^{32}P labeled nucleotide onto the immobilized primer terminus was monitored by visualizing the labeled enzyme-TP covalent complex by resolving the complex on 8% SDS-PAGE followed by PhosphorImaging.

Preparative Scale Modification of NSSB by [^3H]-FSBA and Tryptic Digestion of Modified Protein.

Modification of HCV NSSB with FSBA was carried out incubating 15 nmol of the enzyme with 1 mM [^3H]-FSBA or unlabeled FSBA at 37°C in the incubation mixture in a final volume of 1 mL, as described above. After 1 h of incubation, 10 mM DTT was added to stop the reaction. For HPLC analysis, the modified protein was precipitated by adding TCA (10% final) and washed twice with 0.5 mL of acetone to remove residual TCA. The protein pellet was first dissolved in 8 M urea in 100 mM sodium bicarbonate buffer, pH 8.0, then diluted to 2 M urea in the same buffer. Trypsinization was done at 37°C at a trypsin-to-HCV NSSB ratio of 1:50. The trypsinized protein was adjusted to 0.1% TFA and resolved on HPLC. HCV NSSB without FSBA treatment was processed and trypsinized in a manner similar to that for HPLC analysis and considered as the control for MALDI/MS analysis, the FSBA-modified enzyme and unmodified control enzyme were resolved on 8% SDS-PAGE. The gel was stained with 0.1% Coomassie brilliant blue R250 in 10% acetic acid, 50% methanol, and 40% H₂O for 10 min. The gel was destained overnight in the same solution

except the dye. The protein bands were excised and processed for MALDI/MS analysis.

HPLC Purification of Tryptic Peptides. Tryptic peptides were resolved on C18 reverse-phase HPLC column (Phenomenex Kinetex XB). The photodiode array detector was set to monitor the eluants at 220 and 254 nm. Elution was programmed by a linear gradient of solvent A: (H₂O, 0.1% TFA) into solvent B: (acetonitrile) over 10 min at 0–1% solvent B. Then a linear gradient was run from 1–50% solvent B for 40 min and 50–100% solvent B for 30 min with a flow rate of 1.5 mL/min. The sample collector was set to collect 1.5 mL fractions. An aliquot of each fraction was counted for ³H radioactivity in a liquid scintillation counter. The peptide peaks with significant radioactivity were further purified on HPLC C4 reverse-phase column (Delta Pak, 300 Å, 3.9 mm × 15 cm) and subjected to LC/MS/MS analysis.

MS Analysis of HCV NS5B Covalently Modified with FSBA. For MALDI/MS analysis, the excised gel bands were dried in Speedvac and *in situ* trypsin digested at 37 °C for 16 h. MS analyses were acquired using the MALDI-TOF/TOF technique on an Applied Biosystems 4800 MALDI-TOF/TOF mass spectrometer. Matrix solution contained 3.0 mg/mL α -cyano-4-hydroxycinnamic acid as a matrix. The spectra were internally calibrated using bradykinin and ACTH (18–39, human (CLIP) as an internal standard; protonated, mono-isotopic masses of 1060.569 and 2465.199 Da, respectively. Comparative MALDI analysis was done on a peptide fingerprint map (PFM) over the 600–4500 Da mass range in reflector positive mode, summing 2000 laser shots. The spectra of control and modified samples were compared to determine likely candidates for SBA-modified peptides. The complete protein sequence was entered into an in-house database to permit matching of the peptide. Modification of peptides by SBA (sulfonylbenzoyl adenosine; +433.08 Da) and the product of ester hydrolysis of FSBA, sulfonylbenzoic acid (SB; +183.983 Da), were entered as user-defined variable modifications.

LC-MS/MS analyses of HPLC-purified peptides were acquired on a Thermo Scientific LTQ Orbitrap equipped with a Waters Nanoacquity UPLC system using a Waters Symmetry C18 180 μ m × 20 mm trap column and a 1.7 μ m, 75 μ m × 250 mm nanoacquity UPLC column (35 °C) for peptide separation. Trapping was done at 15 μ L/min in 99% buffer A (water, 0.1% formic acid) for 1 min. Peptide separation was done in a two-step gradient of buffer B (CH₃CN, 0.075% formic acid) to buffer A at a flow rate of 300 nL/min. The elution was programmed with 5% buffer B, 50% buffer B at 50 min, and 85% buffer B at 51 min. MS was acquired in the Orbitrap using 1 microscan over the range of 400–2000 *m/z* at 30000 resolution and a maximum inject time of 900 ms, followed by six data-dependent MS/MS acquisitions in the ion trap. MS/MS spectra were searched in-house using the Mascot algorithm for uninterpreted MS/MS spectra after using the Mascot Distiller program to generate Mascot compatible files.⁴⁶ The Mascot Distiller program combines sequential MS/MS scans from profile data that have the same precursor ion. A charge state of +2 and +3 is preferentially located with a signal-to-noise ratio of 1.2 or greater; a peak list is generated for database searching. The data were searched against a sequence-specific database using a peptide tolerance of ± 15 ppm, MS/MS fragment tolerance of ± 0.6 Da, and peptide charges of +2, +3, or +4. The modifications by SBA (+433.069 Da) and SB (+183.983 Da) were investigated.

Molecular Docking. We used induced-fit docking (IFD) workflow of Schrodinger Suit (Schrodinger LLC, New York, NY) for this purpose. The crystal structure of NS5B bound to GTP (PDB entry 1GX5) at the allosteric site was used for docking FSBA to NS5B. The crystal structure was prepared using the protein preparation workflow in the Schrödinger Maestro modeling package version 9.2. The GTP, catalytic metals (Mn²⁺), and triphosphate moieties were removed from the crystal structure during protein preparation workflow. The structure of FSBA to be docked into the crystal structure was generated as follows. The initial structure of FSBA was obtained from PubChem (pubchem.ncbi.nlm.nih.gov) entry number 133129 in sdf format. The 3D conformations of FSBA from this structure were generated by the Epic and LigPrep ligand preparation protocols of the Schrodinger Suit incorporated in the Maestro 9.2 molecular modeling environment. Two separate induced-fit docking runs were carried out. In the first run, the docking was done using the centroid out at the centroid of K491 residues; in the second run, the centroid of Y382 atoms was considered. The box size was 50 Å³ in each case.

RESULTS

Binding Affinity of FSBA to HCV NS5B. FSBA, a chemically reactive analogue of ATP, has affinity for enzymes that use ATP as a substrate. Therefore, by measuring fluorescence quenching (FQ) of the enzyme in the presence and absence of FSBA, we tested whether FSBA can bind to HCV NS5B. The binding of NTPs to HCV NS5B significantly reduces the fluorescence emission intensities of the enzyme at 330 nm when excited at 280 nm.^{47,48} We therefore incubated a fixed concentration of HCV NS5B with varying concentrations of FSBA and measured the fluorescence emission between 300 and 420 nm. The emission fluorescence maximum was noted at 330 nm, which was significantly quenched in the presence of FSBA (Figure S1A). As shown, the increase in FQ was correlated with and proportional to the increase in FSBA concentration. At as low a level as 62 μ M of FSBA, the fluorescence emission was reduced by 12%, while at 1 mM concentration of the analogue, 70% reduction in the emission intensity was noted (Figure S1B). We could not determine the binding affinity of this analogue since it is chemically reactive and forms a covalent bond with amino acid residue at its binding site.

Inactivation of RdRp Activity of HCV NS5B by FSBA. We noted that FSBA, being an ATP analogue, rapidly binds to the enzyme and quenches its emission fluorescence, as does NTP substrate.⁴⁸ To examine the effect of FSBA on HCV NS5B activity, we measured the RdRp activity of the enzyme in the presence of increasing concentrations of FSBA (Figure 2A). We observed that FSBA binding to the enzyme inactivated its RdRp activity. Approximately 70% inactivation of RdRp activity was noted at 0.6 mM concentration of FSBA. At higher concentration of the analogue (1 mM), the inactivation was only marginally increased probably due to its decreased solubility of the analogue beyond 1 mM concentration. We then examined the inactivation pattern of the enzyme as a function of both time of incubation and FSBA concentration. We incubated HCV NS5B with 0.25 mM, 0.5 mM, and 1 mM FSBA at 4 °C and at 5, 10, 20, 40, and 60 min, withdrew an aliquot of sample and assayed it for RdRp activity (Figure 2B). We noted 15% inactivation of the RdRp activity of the enzyme when it was incubated with 0.25 mM FSBA for 20 min, but 20–

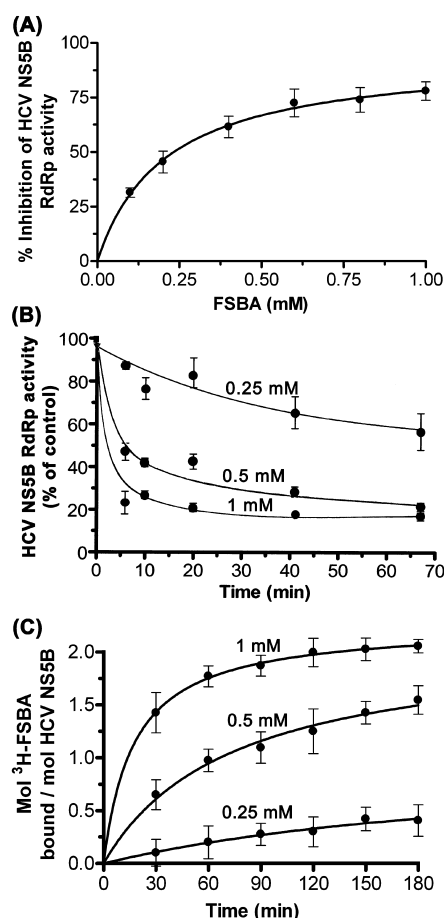


Figure 2. Inactivation of RdRp activity of HCV NSSB by FSBA. (A) RdRp activity assay of HCV NSSB was done in the presence of increasing concentrations of FSBA. The reaction was carried out for 60 min and percent of inactivation of RdRp activity was determined with respect to control. (B) HCV NSSB was preincubated with indicated concentration of FSBA at 4 °C. At indicated time points the samples were withdrawn from the incubation mixture and assayed for RdRp activity. (C) Binding stoichiometry of FSBA to NSSB as a function of FSBA concentration and time of incubation. Four micromolar NSSB was incubated at 30 °C in the presence of an indicated amount of [³H]-FSBA in a final volume of 500 μ L. At indicated time point, aliquots were withdrawn and subjected to ascending paper chromatography followed by quantification of the radiolabeled protein using liquid scintillation counting as described in the Materials and Methods. The GraphPad PRIZM software was applied to plot the data using a nonlinear fit to the data using a hyperbolic function equation ($Y = B_{max}I \cdot X / (K_d + X)$) where B_{max} is the maximal inactivation and K_d is the concentration of ligand required to reach half maximal inactivation or binding of ligand to the enzyme.

30% after 40 min of incubation. At 1 mM concentration of FSBA, enzyme activity was reduced approximately 70% within 10 min of incubation; 80% reduction occurred after 60 min of incubation.

Binding Stoichiometry of FSBA to HCV NSSB. We noted that FSBA being an ATP analogue inactivates the RdRp activity of NSSB and is expected to bind with enzyme in an irreversible manner. Covalent attachment of the [³H]-labeled FSBA to the enzyme was monitored as a function of time and concentration of FSBA (Figure 2C). The covalent attachment of FSBA to the enzyme was found to vary with time and was dependent on the FSBA concentration. At 1 mM concentration

of FSBA, the binding stoichiometry was approximately 2 moles per mole of enzyme after 90 min incubation.

Protection of HCV NSSB from FSBA in the Presence of rNTPs and Different Template-Primers. To determine whether inactivation of HCV NSSB by FSBA can be protected in the presence of nucleotides, or template primer, we preincubated HCV NSSB in the presence of individual NTPs (ATP, GTP, CTP, and UTP), or with template-primer and then supplemented with 0.5 mM FSBA. The reaction mixture was incubated at 4 °C for 1 h and an aliquot of the incubation mixture was assayed for RdRp activity (Table 1). We observed

Table 1. Effect of Various Additions on the FSBA-Mediated Inhibition or Inactivation of RdRp Activity of HCV NSSB^a

additions	RdRp activity (% of control)	
	50 mM NaCl	150 mM NaCl
0.5 mM FSBA	33 \pm 4	35 \pm 8
+ 1 mM ATP	83 \pm 7	82 \pm 6
+ 1 mM GTP	87 \pm 8	86 \pm 8
+ 1 mM CTP	84 \pm 8	82 \pm 5
+ 1 mM UTP	90 \pm 9	87 \pm 8
+ 10 μ g poly rA.rU ₁₂	70 \pm 9	56 \pm 5
+ 10 μ g poly rA.dT ₁₈	83 \pm 6	50 \pm 3
+ 37-mer looped RNA	90 \pm 8	56 \pm 5
+ 10 μ g poly rU.rA ₂₆	35 \pm 5	46 \pm 4

^aReaction mixture was incubated in 100 μ L final volume containing 10 μ M HCV NSSB with the indicated additions in the absence or presence of 0.5 mM FSBA. After 1 h incubation at 4 °C, an aliquot of the incubation mixture was withdrawn and assayed for RdRp activity. The percent of HCV NSSB RdRp activity is expressed with respect to the control. Data represent the mean values (\pm SD) obtained from two independent experiments. The sequence of 37-mer double-stranded RNA looped template primer is shown in Figure 3.

that in the presence of rNTP, poly rA.dT₁₈, 37-mer looped RNA or poly rA.rU₁₂ template primer, the RdRp activity of the enzyme is protected from FSBA, but similar protection was not observed in the presence of poly rU.rA₂₆. The protection of enzyme activity in the presence of poly rA.dT₁₈, 37-mer looped RNA and poly rA.rU₁₂ template primers can be explained since incoming nucleotide with these template primers is UTP; therefore, binding of the ATP analogue is expected to be excluded. In the presence of poly rU.rA₂₆, enzyme activity was not protected from FSBA because incoming nucleotide with this template primer is ATP.

We further observed that the protection of the enzyme activity from FSBA in the presence of TP is significantly reduced at 150 mM salt concentration but salt had no effect on the protection in the presence of rNTP substrate. This may be possible that binding of double-stranded nucleic acid substrate to HCV NSSB requires low ionic strength. To examine this possibility we incubated the enzyme with 5'-³²P labeled 37-mer double-stranded looped RNA template primer as well as with poly rA.5'-³²P-dT₁₈ in the presence of increasing salt concentrations. The incubation mixture was UV irradiated and the resulting ³²P labeled E-TP complexes were resolved by SDS-PAGE. The results shown in Figure 3 indicate that HCV NSSB efficiently binds to heteromeric 37-mer dsRNA looped TP (Figure 3A) and homopolymeric double stranded nucleic acid substrate (Figure 3B) at 50 mM salt concentration. The formation of enzyme-TP binary complex was reduced to 50% and 75% at 100 mM and 150 mM salt, respectively, and nearly

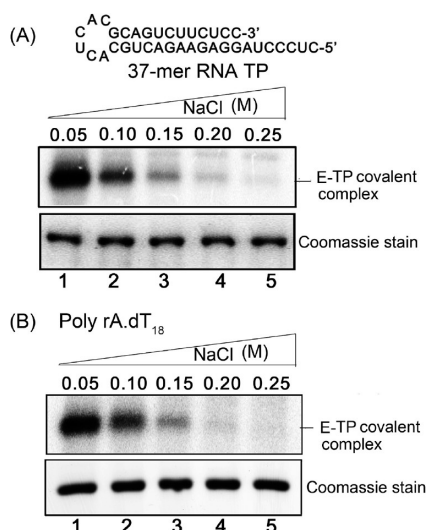


Figure 3. Effect of salt concentration on the binding of double-stranded RNA TP to HCV NSSB. HCV NSSB was incubated with either $S^{32}P$ labeled 37-mer self-annealing RNA template primer (A) or with poly rA. $S^{32}P$ -dT₁₈ (B) in the presence of indicated salt concentration on ice for 20 min and then UV irradiated as described in the Materials and Methods. The enzyme-TP binary covalent complexes were resolved by SDS-PAGE. The E-TP covalent complex was visualized by autoradiography and the protein band was stained by Coomassie blue.

abolished at or above 200 mM salt concentration. These results suggest that template primer binding to the enzyme is drastically reduced even at physiological salt concentration and therefore offers no protection to the enzyme from FSBA mediated inactivation. This could be due to low electropositive potential in the template primer binding track of the enzyme. Lohman et al. have reported 80% reduction in RdRp activity of HCV NSSB at 100 mM KCl and 50% reduction at 150 mM NaCl concentration. This reduction in the activity could be due to low binding of double-stranded nucleic acid substrates used in their assay system.⁴⁹

We further noted that high salt concentrations have no effect on the protection of enzyme activity in the presence of rNTP substrates. This could be due to the hydrophobic nature of rNTP binding pocket which may be insensitive to high salt concentration. To examine this hypothesis, we incubated HCV NSSB with unlabeled 37-mer looped RNA TP and UV irradiated to covalently cross-link with the enzyme. An aliquot of the enzyme-TP binary complex was incubated with first incoming nucleotide, $\alpha^{32}P$ UTP, at different salt concentrations ranging from 50 mM to 1 M in the RdRp reaction buffer. The reaction mixture was incubated at 37 °C for 30 min and then resolved by SDS-PAGE. The results shown in Figure 4 indicate that enzyme-TP binary complex was able to incorporate a single nucleotide onto the immobilized primer terminus of the double-stranded TP even at 1 M salt concentration suggesting the salt-resistant hydrophobic nature of the nucleotide binding pocket.

Comparison of Tryptic Peptides and LC/MS/MS Analysis of Affinity-Labeled Peptides. To identify the binding site of FSBA, we did tryptic peptide mapping of the [3H]-FSBA-modified enzyme, using HPLC. We used unmodified enzyme as the control. The tryptic digests of the modified and unmodified enzyme were separated by HPLC using a C₁₈ reverse-phase column. The eluants were monitored at 220 and

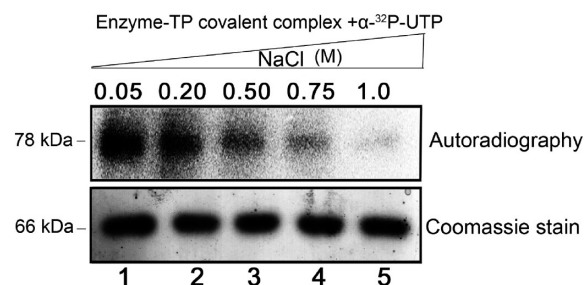


Figure 4. Effect of salt concentration on the incorporation of a single nucleotide onto the immobilized primer terminus of enzyme-TP covalent complex. The unlabeled 37-mer self-annealing RNA TP was covalently cross-linked with the enzyme by UV irradiation. An aliquot of the E-TP covalent complex was incubated with $\alpha^{32}P$ UTP in the presence of indicated salt concentration as described in the Materials and Methods. After 30 min incubation at 37 °C, the reaction mixture was subjected to 8% SDS-PAGE. The incorporation of a single nucleotide on to the immobilized primer terminus of E-TP covalent complex was visualized by autoradiography and protein band by Coomassie blue staining.

254 nm to detect the concurrence of SBA-labeled peptides; the peptide labeled with SBA moiety was expected to give relatively high absorbance at 254 nm. Since HCV NSSB was modified by [3H]-FSBA, we also monitored the eluants for radioactivity. The results shown in Figure S2B indicate the absorbance of tryptic peptides monitored at 254 nm to detect SBA linked peptides. As shown, three distinct radioactive peaks were eluting at Rt 20.3, 23.6, and 36.8 min. The radioactive peak eluting at Rt 20.3 was unreacted free FSBA since free FSBA also eluted at the same position. The radioactive peaks eluted at 23 and 36 min were found to be associated with peptides (Figure S2B). Both of these peptides were conspicuously absent in the control without modification (Figure S2A). We also analyzed tryptic peptides of the enzyme modified by FSBA in the presence of ATP (Figure S2C). We noted that both of the radioactive peptide peaks eluting at 23 and 36 min were significantly reduced, suggesting that in the presence of ATP the modification of enzyme by FSBA is significantly protected. We further purified these peptides and subjected them to LC/MS/MS analysis to identify the peptides and site of modification. The LC/MS/MS analysis showed that the peptide eluted at 23 min spanned residues 33–43 in the primary sequence of HCV NSSB, with Y38 as the modification site. The peptide peak eluted at 36 min was found to contain two peptides spanning residues 381–386 and 491–498, with Y382 and K491 as the respective modification sites (Table 2). A representative MS/MS fragmentation pattern of peptide eluting at 36 min is shown in Figure 5.

Characterization of the FSBA Labeling Site Using MALDI-TOF/TOF. To confirm the FSBA modification site in HCV NSSB, we used highly sophisticated MALDI-TOF/TOF analysis of the tryptic digest of FSBA-modified HCV NSSB. Both FSBA-modified enzyme and unmodified control were subjected to SDS-PAGE. The protein bands were excised from gels and processed for in situ trypsin digestion. The digested samples were then analyzed on MALDI-TOF/TOF to acquire the MS data. The MS data of the FSBA-modified sample was compared with the unmodified control (Figure 6). Microscopic analysis of the MS spectra showed two major peptides with masses of 998.43, 1311.63, and a minor peptide of 1500.60 Da in the FSBA-modified sample which were absent in the control (Figure 6). Further MS analysis of two major peptides showed

Table 2. Peptide Modification by FSBA as Determined by LC/MS/MS and MALDI-TOF/TOF

Peptide	(<i>m/z</i>)	N5SB residue with modification	ATP prevents cross-linking ^c	Target residue	Comments
1	998.43 ^b	³⁸¹ VYYLTR ³⁸⁶ SB	yes	Tyr382	Tyr382 is located on the β7 strand at the interface of thumb and palm
2	1246.50 ^a	³⁸¹ VYYLTR ³⁸⁶ SBA			
3	1311.63 ^{a,b}	⁴⁹¹ KLGVPPLR ⁴⁹⁸ SBA	yes	Lys491	Lys491 is located on the αS helix in the thumb domain whereas Tyr38 is located on the β2 finger loop connecting thumb and finger domain
4	1500.60 ^{a,b}	³³ HHNMVYATTSR ⁴³ SB	yes	Tyr38	

^aHPLC purified peptides were analyzed by LC/MS/MS. ^bThe FSBA-modified HCV N5SB was resolved over 8% SDS-PAGE and subjected to in situ trypsin digestion, followed by MALDI-TOF/TOF analyses. Peptide modified at a particular position by SBA or SB is shown as identified by MS fragmentation pattern. The molecular masses of SBA and BA were calculated as 433.08 and 183.98 Da, respectively. ^cHCV N5SB was incubated with 1 mM ATP before the addition of FSBA to the labeling reaction. The protein was TCA precipitated and digested by trypsin, followed by HPLC analyses. Comparisons of tryptic peptide profiles of the samples in the presence and absence of ATP were acquired where “yes” indicates the protection of HCV N5SB from FSBA-mediated modification (see Figure S2 for details).

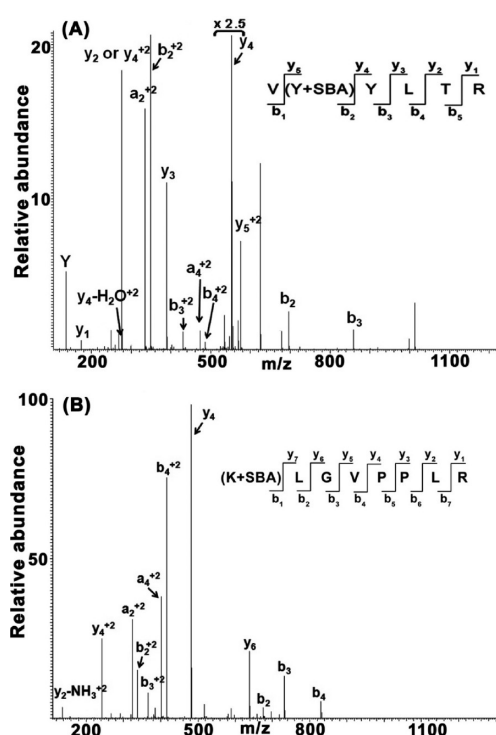


Figure 5. Tandem mass spectrometry of FSBA modified peptides. (A) The representative MS/MS spectrum of triply charged ion at *m/z* 1246.50 shows the peptide ³⁸¹VYYLTR³⁸⁶ modified by SBA at Tyr382. (B) The MS/MS spectrum of the triply charged ion at *m/z* 1311.63 shows the peptide ⁴⁹¹KLGVPPLR⁴⁹⁸ modified by SBA at Lys491. Fragmentation patterns of the peptides are shown in the inset.

that the 998.43-Da peptide corresponded to residues 381–386 and contained Y382 as the modification site while the 1311.63 Da peptide spans residues 491–498 with K491 as the site of modification. The minor peptide of 1500.60 Da spans residue 33–43 with Y38 as the modification site (Table 2). The peptide mass of 1311.63 Da represents an additional mass of 433.08 Da due to sulfonylbenzoyl adenosine (SBA) attached with the peptide, while the peptides having masses of 998.43 Da and 1500.60 Da represent an additional mass of 183.98 Da due to

the attachment of the sulfonylbenzoyl moiety (SB) of SBA.⁴³ This might be due to ester hydrolysis of the SBA moiety during sample preparation, in which only the SB moiety remains intact, with the modified residue showing a mass increase of 183.98 Da. In MALDI-MS experiments, we found the coverage of 89% of the primary sequence of HCV N5SB obtained by MS analysis (Figure 7).

Mutational Analysis of the Identified Residues. Since all three identified sites are protected from modification from FSBA in the presence of ATP, it is likely that they are part of the NTP channel or NTP binding pocket of the enzyme. We therefore carried out site-directed mutagenesis to generate Y38A, Y382A, and K491A mutants of the enzyme. We purified the mutant enzymes and examined their RdRp activity. As shown in Figure 8A, Y382A and K491A had severely impaired polymerase activity, while Y38A remained unaffected. These results indicate that Y382 and K491 are important residues for catalysis, while Y38 is dispensable. K491 is located in the NTP channel and substitution of the Lys side chain with Ala may perturb the NTP channel.⁵⁰ The Y382 is located on the β16 sheet at the interface of finger and thumb, very close to the suggested primer grip region corresponding to β14–β15.¹⁵

Effect of Y382A and K491A Mutations on the Binding of Template-Primer and ATP Substrate. The reduction in RdRp activity of Y382A and K491A mutants could be due to a defect in either the template primer binding step or at the nucleotide binding step. In order to determine the template primer binding ability of the mutant enzymes, we used a double-stranded 5′-³²P labeled 37-mer self-annealing RNA template primer (Chart S1) to photo-cross-link with the wild type and its mutant derivatives. The results shown in Figure 8B indicated no significant change in the template primer binding ability of both Y382A and K491A mutant enzymes as compared to the wild type enzyme. We then examined their ability to cross-link ATP substrate in the binary (enzyme-ATP) and ternary (enzyme-TP-ATP) complexes. The template primer that we used had 3′ deoxy terminated rA₁₀ primer annealed with rU₁₅ template (rU₁₅/rA₁₀-3′ deoxy) which supports ATP as the incoming nucleotide. The results shown in Figure 8C indicated that both the mutant enzymes were significantly affected in their ability to cross-link ATP in the binary and

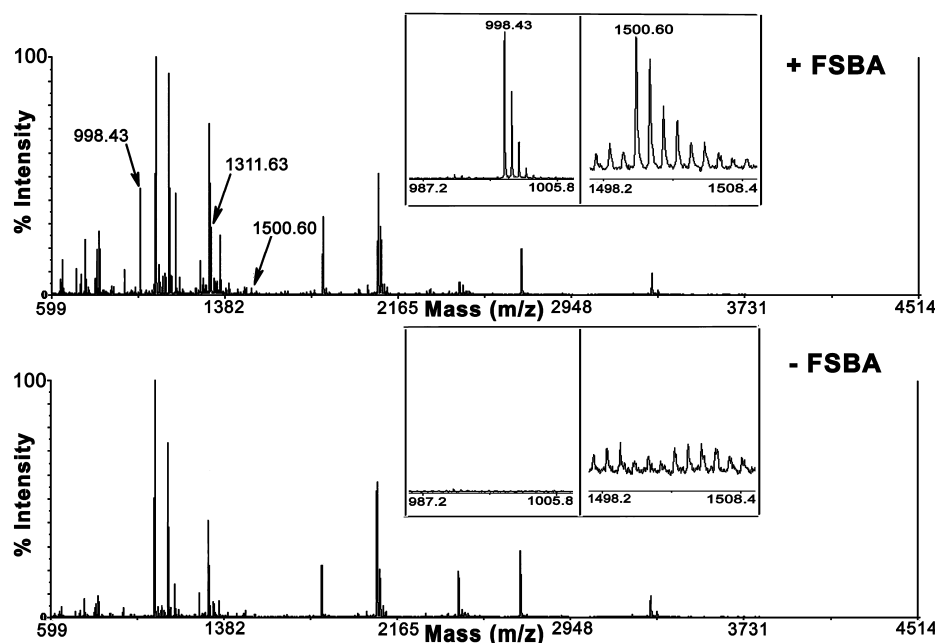


Figure 6. Identification of the FSBA binding sites using MALDI-TOF MS. HCV NSSB (5 μ M) was incubated in the presence and absence of 1 mM FSBA at 37 $^{\circ}$ C for 1 h in a total volume of 100 μ L. After labeling, samples were resolved on 8% SDS-PAGE. The corresponding protein bands were visualized by mild staining. The protein bands were excised and in-gel trypsin digested and analyzed by MALDI-TOF. Comparison of full-scan MS data indicates the modification of the FSBA-treated sample at m/z 998.43, 1311.63, and 1500.60 (indicated by arrow). The inset shows the zoomed modification at m/z 998.43 and 1500.60 as a representative of all three modifications identified. “+ and – FSBA” denotes NSSB treated in the presence and absence of FSBA.

ternary complexes. We further found that extent of reduction in the ATP cross-linking ability of K491A mutant was similar either in the binary and ternary complexes (lanes 3 and 6), whereas reduction in the cross-linking was more pronounced with the Y382A mutant in the ternary complex. The Y382 and K491 may be part of multiple noncovalent interactions/contact points between the ATP and the enzyme molecule. The reduction in the extent of cross-linking of ATP to Y382A and K491A mutants may be due to removal of one of the multiple contact points with ATP in the nucleotide binding pocket.

Molecular Docking of FSBA at the Nucleotide Binding Site of HCV NSSB. The most favorable poses (i.e., the least energy-docking conformer) for two induced-fit docking (IFD) workflows were used for analyses of the binding of FSBA to NSSB (Figure 9A,C). The first IFD complex obtained after docking of FSBA at the centroid of K491 is shown in Figure 9A, displaying specific interactions of FSBA with neighboring amino acid residues. The polar (H-bond) interactions are shown in cyan-dotted lines, while the van der Waals interactions are shown as orange double-dotted lines; the positions of active-site residues (D318, D319, and D220) are included as references. The nitrogen of epsilon amino group of K491 side chain is within interacting distance of 3.4 Å from the fluorosulfonyl group of FSBA. The other important residues that interact in this modeled complex are F145, K155, S367, R386, D387, and T390. Bressanelli et al. showed that R158, S367, R386, and T390 interact with one of the triphosphates in the crystal structure of NSSB.¹⁸ The position of some of these interacting residues can be clearly seen in the surface view of the putative NTP channel (Figure 9B). These residues have been proposed to be part of the priming site.¹⁸ The initiation site residues R48, K51, K151, K155 and R158 have been suggested to be the part of NTP-tunnel.¹⁸ In our complex, residues K155 interact with FSBA. Therefore, this complex can

be considered to represent a combination of priming-site and initiation-site complexes described previously.

The second IFD complex, shown in Figure 9C, was obtained by docking FSBA near Y382. In this complex, the FSBA appears to be stabilized by polar (H-bond), van der Waals, and hydrophobic interactions. The distance between the oxygen atom of Y382 and the fluorosulfonyl group of FSBA is 3.7 Å. Amino acid residues H467, S470, D375, K379, and K209 form H-bond interactions with various moieties of FSBA. G198, E202, and V205 interact through van der Waals interactions. The ring moieties of FSBA are stabilized by hydrophobic interactions with Y383, Y382, and V381. The Y382 located on β 16 in the thumb domain is in the vicinity of the primer grip region (β 14– β 15) on the palm domain. A surface view of this region is shown in Figure 9D. A crystal structure of the ternary complex showing interaction of NTP with these residues is yet to be elucidated.

DISCUSSION

Affinity labeling of enzyme with substrate analogues is frequently used to identify the substrate binding site on the enzyme molecule. FSBA is a unique ATP analogue that has been used to probe the ATP-binding region in ATP-using enzymes.^{35–43} We have used this analogue, as well as its deoxy form (FSBdA), to covalently modify interacting amino acid residues in the polymerase cleft of *E. coli* DNA pol I.³⁶ In our present study, we used FSBA to modify HCV NSSB to identify the nucleotide interacting regions on the enzyme molecule. The electrophilic sulfonyl fluoride moiety of FSBA may readily react and form covalent linkage with Ser, Cys, Lys, Tyr, and His residues located within the region interacting with the incoming nucleotide.^{44,51,52} The position of the fluorosulfonylbenzoyl moiety of the FSBA molecule is similar to that of the triphosphate moiety of ATP; therefore, that moiety is expected

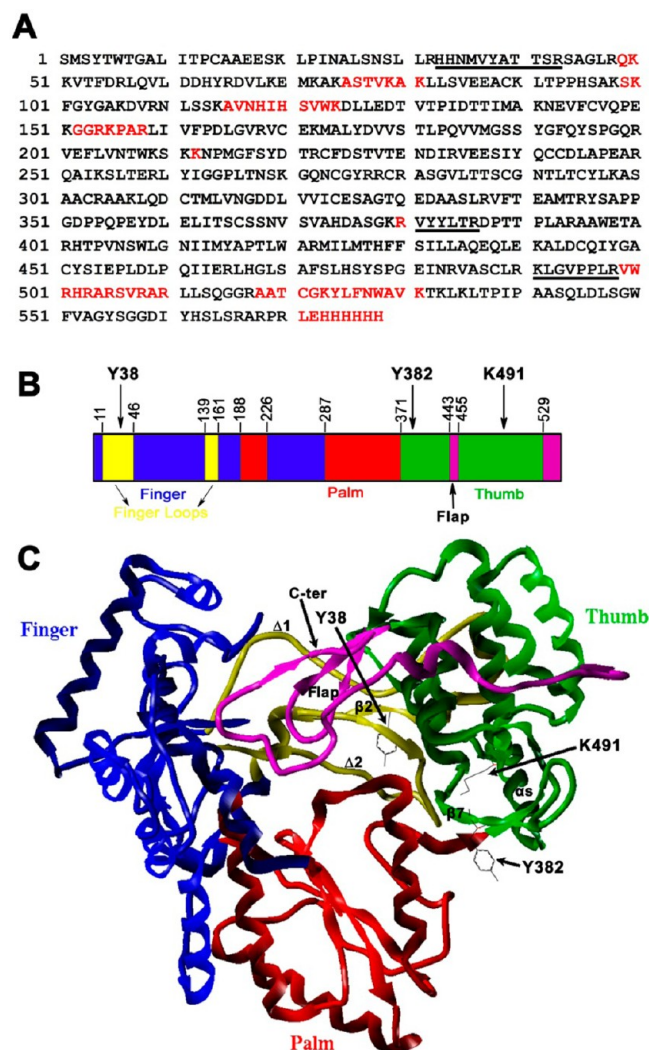


Figure 7. MS coverage and structural representation of NSSB showing FSBA modification sites. (A) MS analysis identified peptides that had coverage of 89% of the sequence of HCV NSSB (bold). The sequence(s) that could not be detected in MS are shown in red. The peptides modified by FSBA and identified by MALDI-MS are underlined. (B) and (C) Blue, red, and green highlight the finger, palm, and thumb subdomains, respectively; yellow represents loops interconnecting the fingers and thumb subdomains; purple represents loops interconnecting the thumb subdomain. (B) and (C) respectively, the linear and three-dimensional representation of NSSB. The identified modification at Y38, Y382, and K491 are shown by the arrow. Y38 is located on the $\beta 2$ finger loop connecting the thumb and finger domains; Y382 is located on the $\beta 7$ strand at the interface of thumb and palm. K491 is positioned on the $\alpha 5$ helix in the thumb domain.

to bind and react with amino acid residues in the vicinity. The reactive sulfonyl fluoride group of enzyme-bound FSBA may form stable covalent adduct with the amino acid residue in the binding site, which could be identified by tryptic peptide profiling followed by mass spectrometry analysis. The relevance of using FSBA to probe the ATP binding site is derived from the fact that its binding to the HCV replicase is protected in the presence of poly(rA)U₁₂ but not in the presence of poly(rU)A₂₆ that supports ATP as the incoming nucleotide. We first confirmed that FSBA binds to HCV NSSB in a concentration-dependent manner with a binding stoichiometry of approximately 2 moles of FSBA per mole of enzyme. We further

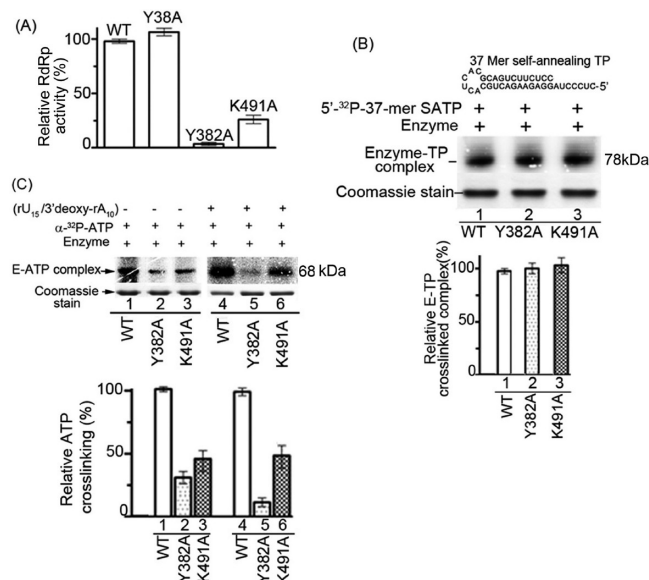


Figure 8. (A) Effect of alanine substitution at position 38, 382, and 491 on the RdRp activity of HCV NSSB. The RdRp activity of the WT and its mutant derivatives (1 μ M) were determined and expressed as percent relative activity with respect to the WT enzyme. (B) Photo-cross-linking of 32 P-labeled RNA template primer to the wild type enzyme and its mutant derivatives. The 5'-[32 P]-labeled 37-mer self-annealing RNA template primer was used as the template primer to cross-link with the WT enzyme and its mutant derivatives. The 32 P labeled 37-mer TP (200 nM) was incubated on ice with 1 μ M of enzyme in a final volume of 50 μ L. The mixture was UV irradiated and the cross-linked E-TP covalent complexes were resolved by SDS-PAGE and visualized by PhosphorImaging. (C) UV mediated photo-cross-linking of 5'- α - 32 P-ATP to the wild type enzyme and its mutant derivatives in the absence and presence of template primer. The wild type enzyme and its mutant derivatives were photo-cross-linked with [α - 32 P]-ATP in the absence of template primer (lanes 1–3) or in the presence of rU₁₅rA₁₀ template primer with 3'-deoxy terminated primer terminus (lanes 4–6). The cross-linked complex was resolved on SDS-PAGE and visualized by PhosphorImaging.

observed that binding of FSBA to HCV NSSB irreversibly inactivates the RdRp activity of the enzyme. Inactivation of the enzyme was readily protected in the presence of NTP, suggesting that reactive sites may be located within the region interacting with NTP substrate. The crystal structure of HCV NSSB soaked with rCTP, rGTP, and rATP in the presence of Mn²⁺ displayed density only for the triphosphate moiety of the nucleotide bound to two metal ions.¹⁸ This indicated that all the NTPs, specifically their triphosphate moieties share the same binding site on the enzyme molecule. Since the reactive fluorosulfonyl group of FSBA is positioned similar to the triphosphate moiety of NTP, its reactivity with the enzyme is protected in the presence of any of the four NTPs. In contrast, in the presence of template primer, the binding of individual NTPs is guided by the template base and thus offering protection to the enzyme in the presence of template primers that do not support ATP as the incoming nucleotide.

However, protection offered by poly(rU)A₂₆ template primer was significantly reduced at 150 mM salt concentration suggesting the double-stranded template-primer binding to the enzyme may be highly sensitive to salt concentration. It has earlier been proposed that the wild type HCV replicase cannot accommodate double-stranded nucleic acid substrate due to close interaction between fingertips and thumb as well as due to

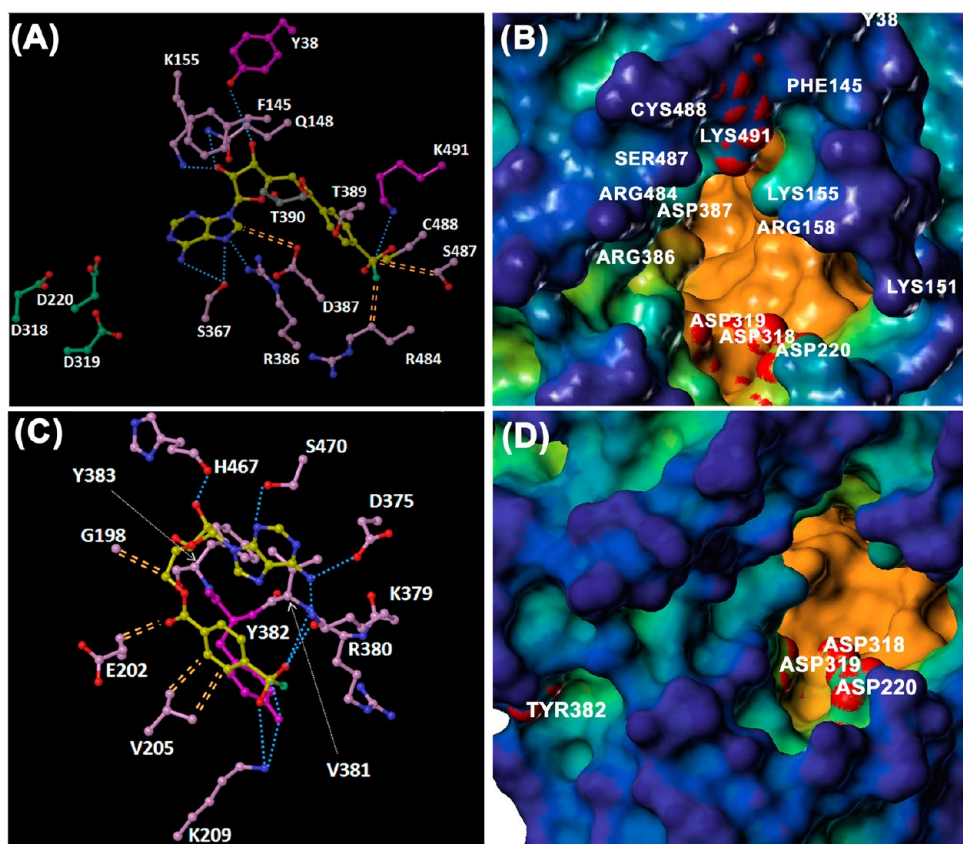


Figure 9. Molecular docking of FSBA at the nucleotide binding site in HCV NSSB. The induced-fit docking of FSBA with NSSB was done using the workflow of a Schrodinger modeling package version 9.2 (Schrodinger LLC., New York, NY). The crystal structure of GTP-bound HCV NSSB (PDB entry 1GX5; (13)) was used for docking of FSBA near LYS491 (A) as well as TYR382 (C). The oxygen of hydroxyl group of TYR382 and nitrogen of epsilon amino group of LYS491 are, respectively, 3.7 Å and 3.4 Å away from the fluorosulfonyl group of FSBA. The van der Waals interactions of FSBA with the neighboring residues are shown as orange double-dotted lines; polar (H-bonding) interactions are shown as cyan-dotted lines. FSBA and target residues are shown as yellow and magenta, respectively. Surface representation of the NTP tunnel showing the position of LYS491 (B) and TYR382 (D). The NSSB residue (protein data bank code 1NB7), which was devoid of RNA and metal, was prepared in Sybyl8.1 with MOLCAD probe radius 1.4 Å (type: cavity depth). The residues LYS491 and TYR382 and the catalytic residues (ASP220, ASP318, and ASP319) are shown in red.

protruding beta flap (amino acid residues from 443 to 454) from the thumb domain into the catalytic cleft.⁵³ We noted that binding of double-stranded RNA substrate to the enzyme requires low salt concentration. HCV NSSB efficiently binds to the dsRNA substrates (poly rA.dT₁₈ and 37-mer RNA TP) at 50 mM salt concentration. At or above 100 mM salt concentration, the formation of enzyme–TP binary complex is drastically reduced (Figure 3). This could be the reason for the reported 80% reduction of RdRp activity with poly rC-oligo dG at 100 mM KCl and 50% reduction at 150 mM NaCl concentrations.⁴⁹ It is possible that at higher salt concentration, the hydrophobic interaction between finger tips and thumb may be strong enough to keep the cleft in closed conformation and thus not accessible for binding to dsRNA substrate. In contrast, at lower salt concentration, the reduced hydrophobic interaction between fingertips and thumb may allow the polymerase cleft to breath and open up to accommodate dsRNA substrate. Another possibility of salt sensitivity could be low electropositive potential of the RNA binding track responsible for dsRNA binding.

Most interestingly, the addition of a single nucleotide onto the immobilized primer terminus of the cross-linked template primer is highly resistant to high salt concentration. As illustrated in Figure 4, the addition of $\alpha^{32}\text{P}$ -UTP onto the

cross-linked 37-mer dsRNA TP could be seen even at 1 M salt concentration. This observation indicates that binding of dsRNA template primer to HCV NSSB was specifically in the primer extension mode and therefore protected FSBA mediated modification of the enzyme. Since both poly rA.rU₁₂ and poly rA.dT₁₈ template primers allow UTP as the incoming nucleotide, the binding of the ATP analogue is expected to be excluded. In contrast, poly rU.rA₂₆ did not protect the enzyme from FSBA because incoming nucleotide with this template primer is ATP.

HPLC analysis of the tryptic digest of HCV NSSB modified with FSBA in the absence and presence of ATP demonstrated the presence of three distinct affinity-labeled peptides, which were protected from modification in the presence of ATP. LC/MS/MS analysis of the HPLC-purified affinity-labeled peptide identified the peptides spanning residues 33–43, 381–386, and 491–498, each containing a unique site of modification at Tyr38, Tyr382, and Lys491, respectively. However the MALDI-MS analysis of the tryptic digest of FSBA-modified HCV NSSB, detected two major peptides and a minor peptide that were absent in the tryptic digest of unmodified control. Further MALDI-TOF/TOF analysis of these peptides identified Tyr382 and Lys491 as the major sites and Tyr38 as the minor site of modification.

		38		382		491
pdb1gx5	31	TRHH--NXVWATTSRSA	374	HDMSGKGVYMLTRDE	489	LRKLGVPPLRWVH
pdb1sh0	31	TFEGTDEPALLGGKDER	352	RITAKLREYGLKFTIR	460	ELKEGGDFYVPEQ
pdb1s4f	34	IREGRGRNIYNHQIGT	405	FCSHTPVFVRWSNT	523	NLSLSLTGVWT-EH
pdb1u09	21	IAETVAEGVENPEFGPA	352	AKKPHFKSLCQTITP	444	E-PFQGI-FETPSY
pdb3ddk	25	LEPSVFEQVEEGKKEPA	343	ILAEAGEGYGLIMTP	463	-----
pdb1ra6	25	LEPSAEHYVEEGKKEPA	342	ILAQSGEDYGLTMTTP	462	-----

Figure 10. The structural alignment of RNA-dependent RNA polymerases of RNA viruses based on conserved structural elements. The PDB codes are 1gx5, HCV NSSB; 1sh0, Norwalk virus (Triclinic); 1s4f, bovine viral diarrhea virus (BVDV); 1u09, foot-and-mouth disease virus (FMDV); 3ddk, Cocksackie virus; and 1ra6, Polio virus.

Since Y38 is located on the surface of the $\Delta 1\text{-}\alpha\text{-}\beta 2$ finger loop which closes the polymerase cleft, we believe that the finger loop containing Y38 may undergo repositioning during FSBA entry into the polymerase cleft and thus transiently exposing Y38 to FSBA. Bressanelli et al. have shown that soaking the HCV NSSB crystal with GTP identified six amino acid residues on the surface that make direct water-mediated contact with the nucleoside moiety of the bound nucleotide.¹⁸ The position of Tyr38 on the $\Delta 1\text{-}\alpha\text{-}\beta 2$ loop and its interaction with FSBA suggest that it may be part of the surface binding site for the nucleotide and thus may not be an essential residue for the RdRp activity of the enzyme. This was confirmed by our site-directed mutagenesis studies in which Tyr side chain at position 38 was substituted with Ala; the resulting Y38A mutant was found to display wild-type activity. The Lys491 that we have identified as the reactive site of FSBA is located on the $\alpha 5$ helix in close proximity to the active site cavity of the enzyme. Deval et al. have proposed that Lys491 is positioned in the NTP channel;⁵⁰ its interaction with NTP analogue, FSBA, is in agreement with this contention. Lys491 seems to be an important but dispensable residue in the NTP channel since K491A mutant retained 25% of the wild-type activity.

FSBA's major interaction was seen with Tyr382, as judged by MALDI-MS analysis of tryptic peptides of the modified HCV NSSB. This residue is located on $\beta 16$ in the thumb, in the vicinity of the putative primer grip $\beta 14\text{--}15$ loop in motif E on the palm domain. In the structure of UTP-bound HCV NSSB, Ser367 in the motif E on the $\beta 14\text{--}\beta 15$ hairpin and Arg386 at the base of the $\beta 16\text{-}\alpha 0$ helix loop have been shown to hydrogen bond with β -phosphate; Thr390, on the $\alpha 0$ helix, hydrogen bonds with the γ phosphate of UTP.¹⁸ Both Arg386 and Tyr382 share the highly conserved motif YYLTRD, which is essential for RdRp activity of the enzyme. Ala substitution at position 386 inactivates RdRp activity of the enzyme.⁵⁰ We found that Tyr382 is also indispensable for the catalytic function of the enzyme, since substitution of Tyr to Ala at this position severely impaired nucleotide binding and the polymerase function of the enzyme (Figure 8). The alignment of three-dimensional structure of RNA-dependent RNA polymerases from other RNA viruses, including Norwalk virus, bovine viral diarrhea virus, foot-and-mouth-disease virus, Cocksackie virus, and Polio virus, showed that structurally both Tyr38 and Tyr382 are fairly conserved, while Lys491 is only moderately conserved (Figure 10).

The induced-fit molecular docking of FSBA at the nucleotide binding domain shows that beside Lys491, which is within interacting distance from FSBA, other residues, including Phe145, Arg158, Lys155, Ser367, Arg386, Asp387, and Thr390, also interact in this modeled complex (Figure 9B). It has been proposed that among these residues Arg158, Ser367, Arg386, and Thr390 are part of the primer-site (P-site) and interact

with the triphosphate moiety of NTP.¹⁸ The second induced fit docking near Tyr382 shows His467, Ser470, Asp375, Lys379, and Lys209 forming H-bond interactions with FSBA, while Tyr383, Tyr382, and Val381 appear to stabilize the ring moieties of FSBA by hydrophobic interactions (Figure 9C) and thus may represent nucleotide binding site in HCV NSSB.

■ ASSOCIATED CONTENT

📄 Supporting Information

Sequences of synthetic oligomeric DNA and template primers, and fluorescence quenching data. This material is available free of charge via the Internet at <http://pubs.acs.org>.

■ AUTHOR INFORMATION

Corresponding Author

*Tel.: 973-972-0660. Fax: 973-972-8657. E-mail: pandey@umdj.edu.

Funding

This research was partly supported by grants from NIH/NIAID and NIH/NIDDK (AI073703, DK083560).

Notes

The authors declare no competing financial interest.

■ ACKNOWLEDGMENTS

We gratefully acknowledge Ms. Jean Kanyo for the LC/MS/MS and MALDI/MS analyses of the samples at W. M. Keck Foundation Proteomics facility, Yale University. We also acknowledge access to the HPC facilities and support of the computational biology scientists of IST/High Performance and Research Computing at UMDNJ, Newark.

■ ABBREVIATIONS USED

HCV, hepatitis C virus; SDS-PAGE, sodium dodecyl sulfate polyacrylamide gel electrophoresis; DTT, dithiothreitol; TP, template primer; dsRNA, double-stranded RNA; Poly (rA). (dT)₁₈, polyriboadenylic acid annealed with (oligodeoxythymidylic acid)₁₈; RdRp, RNA-dependent RNA polymerase; FSBA, 5'-*p*-fluorosulfonylbenzoyladenosine; SBA, sulfonylbenzoyladenosine; IMAC, immobilized metal affinity chromatography; Ni-IDA, nickel-iminodiacetic acid; FPLC, fast protein liquid chromatography; HPLC, high pressure liquid chromatography; LC MS/MS, liquid chromatography coupled with MS/MS; MALDI-TOF, matrix assisted laser desorption ionization time-of-flight mass spectroscopy; BSA, bovine serum albumin; NBD, nucleotide binding domain; IFD, induced-fit docking

■ REFERENCES

- (1) Freeman, A. J., Marinos, G., Ffrench, R. A., and Lloyd, A. R. (2001) Immunopathogenesis of hepatitis C virus infection. *Immunol. Cell Biol.* 79, 515–536.
- (2) Chien, D. Y., Choo, Q. L., Tabrizi, A., Kuo, C., McFarland, J., Berger, K., Lee, C., Shuster, J. R., Nguyen, T., Moyer, D. L., et al.

- (1992) Diagnosis of hepatitis C virus (HCV) infection using an immunodominant chimeric polypeptide to capture circulating antibodies: reevaluation of the role of HCV in liver disease. *Proc. Natl. Acad. Sci. U.S.A.* 89, 10011–10015.
- (3) Manns, M. P., McHutchison, J. G., Gordon, S. C., Rustgi, V. K., Shiffman, M., Reindollar, R., Goodman, Z. D., Koury, K., Ling, M., and Albrecht, J. K. (2001) Peginterferon alfa-2b plus ribavirin compared with interferon alfa-2b plus ribavirin for initial treatment of chronic hepatitis C: a randomised trial. *Lancet* 358, 958–965.
- (4) Feld, J. J., and Hoofnagle, J. H. (2005) Mechanism of action of interferon and ribavirin in treatment of hepatitis C. *Nature* 436, 967–972.
- (5) Palumbo, E. (2011) Pegylated interferon and ribavirin treatment for hepatitis C virus infection. *Ther. Adv. Chronic Dis.* 2, 39–45.
- (6) Poynard, T., Yuen, M.-F., Ratziu, V., and Lai, C. L. (2003) Viral hepatitis C. *Lancet* 362, 2095–2100.
- (7) Furman, P. A., Lam, A. M., and Murakami, E. (2009) Nucleoside analog inhibitors of hepatitis C viral replication: recent advances, challenges and trends. *Fut. Med. Chem.* 1, 1429–1452.
- (8) Sherman, K. E., Flamm, S. L., Afdhal, N. H., Nelson, D. R., Sulkowski, M. S., Everson, G. T., Fried, M. W., Adler, M., Reesink, H. W., Martin, M., Sankoh, A. J., Adda, N., Kauffman, R. S., George, S., Wright, C. I., and Poordad, F. (2011) Response-Guided Telaprevir Combination Treatment for Hepatitis C Virus Infection. *N. Engl. J. Med.* 365, 1014–1024.
- (9) Jacobson, I. M., McHutchison, J. G., Dusheiko, G., Di Bisceglie, A. M., Reddy, K. R., Bzowej, N. H., Marcellin, P., Muir, A. J., Ferenci, P., Flisiak, R., George, J., Rizzetto, M., Shouval, D., Sola, R., Terg, R. A., Yoshida, E. M., Adda, N., Bengtsson, L., Sankoh, A. J., Kieffer, T. L., George, S., Kauffman, R. S., and M.D., S. Z. (2011) Telaprevir for Previously Untreated Chronic Hepatitis C Virus Infection. *N. Engl. J. Med.* 364, 2405–2416.
- (10) Poordad, F., McCone, J., Jr., Bacon, B. R., Bruno, S., Manns, M. P., Sulkowski, M. S., Jacobson, I. M., Reddy, K. R., Goodman, Z. D., Boparai, N., DiNubile, M. J., Sniukiene, V., Brass, C. A., Albrecht, J. K., and Bronowicki, J. P. (2011) Boceprevir for untreated chronic HCV genotype 1 infection. *N. Engl. J. Med.* 364, 1195–1206.
- (11) Bacon, B. R., Gordon, S. C., Lawitz, E., Marcellin, P., Vierling, J. M., Zeuzem, S., Poordad, F., Goodman, Z. D., Sings, H. L., Boparai, N., Burroughs, M., Brass, C. A., Albrecht, J. K., and Esteban, R. (2011) Boceprevir for Previously Treated Chronic HCV Genotype 1 Infection. *N. Engl. J. Med.* 364, 1207–1217.
- (12) Zeuzem, S., Andreone, P., Pol, S., Lawitz, E., Diago, M., Roberts, S., Focaccia, R., Younossi, Z., Foster, G. R., Horban, A., Ferenci, P., Nevens, F., Mullhaupt, B., Pockros, P., Terg, R., Shouval, D., van Hoek, B., Weiland, O., Van Heeswijk, R., De Meyer, S., Luo, D., Boogaerts, G., Polo, R., Picchio, G., and Beumont, M. (2011) Telaprevir for retreatment of HCV infection. *N. Engl. J. Med.* 364, 2417–2428.
- (13) Ashfaq, U. A., Javed, T., Rehman, S., Nawaz, Z., and Riazuddin, S. (2011) An overview of HCV molecular biology, replication and immune responses. *Virol. J.* 8, 161.
- (14) Beaulieu, P. L. (2007) Non-nucleoside inhibitors of the HCV NSSB polymerase: progress in the discovery and development of novel agents for the treatment of HCV infections. *Curr. Opin. Investig. Drugs* 8, 614–634.
- (15) Bressanelli, S., Tomei, L., Roussel, A., Incitti, I., Vitale, R. L., Mathieu, M., De Francesco, R., and Rey, F. A. (1999) Crystal structure of the RNA-dependent RNA polymerase of hepatitis C virus. *Proc. Natl. Acad. Sci. U.S.A.* 96, 13034–13039.
- (16) Lesburg, C. A., Cable, M. B., Ferrari, E., Hong, Z., Mannarino, A. F., and Weber, P. C. (1999) Crystal structure of the RNA-dependent RNA polymerase from hepatitis C virus reveals a fully encircled active site. *Nat. Struct. Biol.* 6, 937–943.
- (17) Ago, H., Adachi, T., Yoshida, A., Yamamoto, M., Habuka, N., Yatsunami, K., and Miyano, M. (1999) Crystal structure of the RNA-dependent RNA polymerase of hepatitis C virus. *Structure* 7, 1417–1426.
- (18) Bressanelli, S., Tomei, L., Rey, F. A., and De Francesco, R. (2002) Structural analysis of the hepatitis C virus RNA polymerase in complex with ribonucleotides. *J. Virol.* 76, 3482–3492.
- (19) O'Farrell, D., Trowbridge, R., Rowlands, D., and Jager, J. (2003) Substrate complexes of hepatitis C virus RNA polymerase (HC-J4): structural evidence for nucleotide import and de-novo initiation. *J. Mol. Biol.* 326, 1025–1035.
- (20) Biswal, B. K., Cherney, M. M., Wang, M., Chan, L., Yannopoulos, C. G., Bilimoria, D., Nicolas, O., Bedard, J., and James, M. N. (2005) Crystal structures of the RNA-dependent RNA polymerase genotype 2a of hepatitis C virus reveal two conformations and suggest mechanisms of inhibition by non-nucleoside inhibitors. *J. Biol. Chem.* 280, 18202–18210.
- (21) Di Marco, S., Volpari, C., Tomei, L., Altamura, S., Harper, S., Narjes, F., Koch, U., Rowley, M., De Francesco, R., Migliaccio, G., and Carfi, A. (2005) Interdomain communication in hepatitis C virus polymerase abolished by small molecule inhibitors bound to a novel allosteric site. *J. Biol. Chem.* 280, 29765–29770.
- (22) Ferrer-Orta, C., Arias, A., Escarmis, C., and Verdaguier, N. (2006) A comparison of viral RNA-dependent RNA polymerases. *Curr. Opin. Struct. Biol.* 16, 27–34.
- (23) Ranjith-Kumar, C. T., and Kao, C. C. (2006) Recombinant viral RdRps can initiate RNA synthesis from circular templates. *RNA* 12, 303–312.
- (24) Qin, W., Luo, H., Nomura, T., Hayashi, N., Yamashita, T., and Murakami, S. (2002) Oligomeric interaction of hepatitis C virus NSSB is critical for catalytic activity of RNA-dependent RNA polymerase. *J. Biol. Chem.* 277, 2132–2137.
- (25) Qin, W., Yamashita, T., Shirota, Y., Lin, Y., Wei, W., and Murakami, S. (2001) Mutational analysis of the structure and functions of hepatitis C virus RNA-dependent RNA polymerase. *Hepatology* 33, 728–737.
- (26) Wang, Q. M., Hockman, M. A., Staschke, K., Johnson, R. B., Case, K. A., Lu, J., Parsons, S., Zhang, F., Rathnachalam, R., Kirkegaard, K., and Colacino, J. M. (2002) Oligomerization and cooperative RNA synthesis activity of hepatitis C virus RNA-dependent RNA polymerase. *J. Virol.* 76, 3865–3872.
- (27) Labonte, P., Axelrod, V., Agarwal, A., Aulabaugh, A., Amin, A., and Mak, P. (2002) Modulation of hepatitis C virus RNA-dependent RNA polymerase activity by structure-based site-directed mutagenesis. *J. Biol. Chem.* 277, 38838–38846.
- (28) Chinnaswamy, S., Murali, A., Li, P., Fujisaki, K., and Kao, C. C. (2010) Regulation of de novo-initiated RNA synthesis in hepatitis C virus RNA-dependent RNA polymerase by intermolecular interactions. *J. Virol.* 84, 5923–5935.
- (29) Chinnaswamy, S., Murali, A., and Cai, H. (2010) Conformations of the monomeric hepatitis C virus RNA dependent RNA polymerase. *Virus Adapt. Treat.* 2, 21–39.
- (30) Cramer, J., Jaeger, J., and Restle, T. (2006) Biochemical and pre-steady-state kinetic characterization of the hepatitis C virus RNA polymerase (NSSBDelta21, HC-J4). *Biochemistry* 45, 3610–3619.
- (31) Gu, B., Gutshall, L. L., Maley, D., Pruss, C. M., Nguyen, T. T., Silverman, C. L., Lin-Goerke, J., Khandekar, S., Liu, C., Baker, A. E., Casper, D. J., and Sarisky, R. T. (2004) Mapping cooperative activity of the hepatitis C virus RNA-dependent RNA polymerase using genotype 1a-1b chimeras. *Biochem. Biophys. Res. Commun.* 313, 343–350.
- (32) Shim, J. H., Larson, G., Wu, J. Z., and Hong, Z. (2002) Selection of 3'-template bases and initiating nucleotides by hepatitis C virus NSSB RNA-dependent RNA polymerase. *J. Virol.* 76, 7030–7039.
- (33) Dutartre, H., Boretto, J., Guillemot, J. C., and Canard, B. (2005) A relaxed discrimination of 2'-O-methyl-GTP relative to GTP between de novo and Elongative RNA synthesis by the hepatitis C RNA-dependent RNA polymerase NSSB. *J. Biol. Chem.* 280, 6359–6368.
- (34) Howe, A. Y., Cheng, H., Thompson, I., Chunduru, S. K., Herrmann, S., O'Connell, J., Agarwal, A., Chopra, R., and Del Vecchio, A. M. (2006) Molecular mechanism of a thumb domain hepatitis C virus nonnucleoside RNA-dependent RNA polymerase inhibitor. *Antimicrob. Agents Chemother.* 50, 4103–4113.

- (35) Pandey, V. N., Kaushik, N. A., Pradhan, D. S., and Modak, M. J. (1990) Template primer-dependent binding of 5'-fluorosulfonylbenzoyldeoxyadenosine by *Escherichia coli* DNA polymerase I. Identification of arginine 682 as the binding site and its implication in catalysis. *J. Biol. Chem.* 265, 3679–3684.
- (36) Pandey, V. N., and Modak, M. J. (1988) Affinity labeling of *Escherichia coli* DNA polymerase I by 5'-fluorosulfonylbenzoyladenosine. Identification of the domain essential for polymerization and Arg-682 as the site of reactivity. *J. Biol. Chem.* 263, 6068–6073.
- (37) Knight, K. L., and McEntee, K. (1985) Affinity labeling of a tyrosine residue in the ATP binding site of the recA protein from *Escherichia coli* with 5'-p-fluorosulfonylbenzoyladenosine. *J. Biol. Chem.* 260, 10177–10184.
- (38) Komatsu, H., and Ikebe, M. (1993) Affinity labelling of smooth-muscle myosin light-chain kinase with 5'-[p-(fluorosulphonyl)-benzoyl]adenosine. *Biochem. J.* 296 (Pt1), 53–58.
- (39) Nelson, J. W., Zhu, J., Smith, C. C., Kulka, M., and Aurelian, L. (1996) ATP and SH3 binding sites in the protein kinase of the large subunit of herpes simplex virus type 2 of ribonucleotide reductase (ICP10). *J. Biol. Chem.* 271, 17021–17027.
- (40) Oudot, C., Jault, J. M., Jaquinod, M., Negre, D., Prost, J. F., Cozzzone, A. J., and Cortay, J. C. (1998) Inactivation of isocitrate dehydrogenase kinase/phosphatase by 5'-[p-(fluorosulfonyl)benzoyl]adenosine is not due to the labeling of the invariant lysine residue found in the protein kinase family. *Eur. J. Biochem.* 258, 579–585.
- (41) Vereb, G., Balla, A., Gergely, P., Wymann, M. P., Gulkan, H., Suer, S., and Heilmeyer, L. M., Jr. (2001) The ATP-binding site of brain phosphatidylinositol 4-kinase PI4K230 as revealed by 5'-p-fluorosulfonylbenzoyladenosine. *Int. J. Biochem. Cell Biol.* 33, 249–259.
- (42) Pitson, S. M., Moretti, P. A., Zebol, J. R., Zareie, R., Derian, C. K., Darrow, A. L., Qi, J., D'Andrea, R. J., Bagley, C. J., Vadas, M. A., and Wattenberg, B. W. (2002) The nucleotide-binding site of human sphingosine kinase 1. *J. Biol. Chem.* 277, 49545–49553.
- (43) Payne, L. S., Brown, P. M., Middleditch, M., Baker, E., Cooper, G. J., and Loomes, K. M. (2008) Mapping of the ATP-binding domain of human fructosamine 3-kinase-related protein by affinity labelling with 5'-[p-(fluorosulfonyl)benzoyl]adenosine. *Biochem. J.* 416, 281–288.
- (44) Colman, R. F., Pal, P. K., and Wyatt, J. L. (1977) Adenosine derivatives for dehydrogenases and kinases. *Methods Enzymol.* 46, 240–249.
- (45) Ivanov, A. V., Korovina, A. N., Tunitskaya, V. L., Kostyuk, D. A., Rechinsky, V. O., Kukhanova, M. K., and Kochetkov, S. N. (2006) Development of the system ensuring a high-level expression of hepatitis C virus nonstructural NSSB and NSSA proteins. *Protein Expr. Purif.* 48, 14–23.
- (46) Hirose, M., Hoshida, M., Ishikawa, M., and Toya, T. (1993) MASCOT: multiple alignment system for protein sequences based on three-way dynamic programming. *Comput. Appl. Biosci.* 9, 161–167.
- (47) Bougie, I., and Bisailon, M. (2003) Initial binding of the broad spectrum antiviral nucleoside ribavirin to the hepatitis C virus RNA polymerase. *J. Biol. Chem.* 278, 52471–52478.
- (48) Bougie, I., Charpentier, S., and Bisailon, M. (2003) Characterization of the metal ion binding properties of the hepatitis C virus RNA polymerase. *J. Biol. Chem.* 278, 3868–3875.
- (49) Lohmann, V., Roos, A., Korner, F., Koch, J. O., and Bartenschlager, R. (1998) Biochemical and kinetic analyses of NSSB RNA-dependent RNA polymerase of the hepatitis C virus. *Virology* 249, 108–118.
- (50) Deval, J., D'Abramo, C. M., Zhao, Z., McCormick, S., Coutsinos, D., Hess, S., Kvaratskhelia, M., and Gotte, M. (2007) High resolution footprinting of the hepatitis C virus polymerase NSSB in complex with RNA. *J. Biol. Chem.* 282, 16907–16916.
- (51) Poulos, T. L., and Price, P. A. (1974) The involvement of serine and carboxyl groups in the activity of bovine pancreatic deoxy-ribonuclease A. *J. Biol. Chem.* 249, 1453–1457.
- (52) Saradambal, K. V., Bednar, R. A., and Colman, R. F. (1981) Lysine and tyrosine in the NADH inhibitory site of bovine liver glutamate dehydrogenase. *J. Biol. Chem.* 256, 11866–11872.
- (53) Hong, Z., Cameron, C. E., Walker, M. P., Castro, C., Yao, N., Lau, J. Y., and Zhong, W. (2001) A novel mechanism to ensure terminal initiation by hepatitis C virus NSSB polymerase. *Virology* 285, 6–11.